THE ASTRONOMICAL JOURNAL, 123:404–412, 2002 January

ABUNDANCES AND KINEMATICS OF FIELD STARS. II. KINEMATICS AND ABUNDANCE RELATIONSHIPS

JON P. FULBRIGHT
Dominion Astrophysical Observatory, Herzberg Institute of Astrophysics, National Research Council of Canada, 5071 West Saanich Road, Victoria, BC V8X 4M6, Canada; Jon.Fulbright@nrc.ca
Received 2000 December 14; accepted 2001 September 28

ABSTRACT

As an investigation of the origin of "α-poor" halo stars, we analyze kinematic and abundance data for 73 intermediate-metallicity stars ($-1 > [Fe/H] \geq -2$) selected from Paper I of this series. We find evidence for a connection between the kinematics and the enhancement of certain element-to-iron ([X/Fe]) ratios in these stars. Statistically significant correlations were found between [X/Fe] and galactic rest-frame velocities (v_{RF}) for Na, Mg, Al, Si, Ca, and Ni, with marginally significant correlations existing for Ti and Y as well. We also find that the [X/Fe] ratios for these elements all correlate with a similar level of significance with [Na/Fe]. Finally, we compare the abundances of these halo stars against those of stars in nearby dwarf spheroidal (dSph) galaxies. We find significant differences between the abundance ratios in the dSph stars and halo stars of similar metallicity. From this result, it is unlikely that the halo stars in the solar neighborhood, including even the "α-poor" stars, were once members of disrupted dSph galaxies similar to those studied to date.

Key words: Galaxy: halo — Galaxy: kinematics and dynamics — Galaxy: stellar content — stars: abundances — stars: Population II

On-line material: machine-readable table

1. INTRODUCTION

Traditionally, the chemical enrichment history of the Galaxy is described to follow the general scenario given by Tinsley (1979). In this scenario, the metal-poor halo stars formed from the ejecta of short-lived Type II supernovae. These events eject material rich in the so-called α-elements (here taken as O, Mg, Si, Ca, and Ti). Observed halo stars, which presumably formed from this gas, preserved this pattern by showing [α/Fe] ratios of $\sim$0.3. About 1 Gyr after the initial burst, Type Ia supernovae began exploding, ejecting Fe-group rich material. This explains the observed drop of the [α/Fe] ratio from the halo value at [Fe/H] ~ -1 to solar at [Fe/H] ~ 0 (Edvardsson et al. 1993; McWilliam 1997).

More recently, studies have found halo stars that do not follow this pattern of α-element enhancement. Carney et al. (1997), King (1997), and Hanson et al. (1998, hereafter H98) all found stars with [α/Fe] ratios lower than what is normally expected for halo stars. The globular clusters Ruprecht 106 and Palomar 12 (Brown, Wallerstein, & Zucker 1997) also show [α/Fe] ratios that are relatively low (for their metallicity) compared with the majority of the halo. The most exceptional case is BD $+80°245$, which shows near-solar [α/Fe] ratios at [Fe/H] ~ -2 (Carney et al. 1997). These ratios suggest a different chemical enrichment history for these stars than for the rest of the halo.

Kinematics may help determine the origin of these stars. Carney et al. (1997) noted that the known metal-poor halo stars with unusual abundances all have high apogalactic radii, while H98 found that more of the stars with lower [Na/Fe] ratios move on retrograde orbits. It should be possible, using the large, self-consistent sample of Fulbright (2000, hereafter F00) to test whether or not stars on extreme orbits demonstrate unusual element abundance ratios.

The F00 data set includes the LTE analysis of 15 elements based on high-resolution, high signal-to-noise (S/N) echelle spectra of 168 stars. These stars were selected primarily by metallicity from lists of known metal-poor stars or by their potential as being subdwarfs from their location on a *Hipparcos*-based color-magnitude diagram. All the observed stars are members of the *Hipparcos* catalog. In addition to these 168 stars, an additional 11 stars with equivalent width measurements from Stephens (1999, hereafter S99) were reanalyzed following the same procedure. The analysis procedure of F00 followed a self-consistent methodology aimed at producing the most accurate abundance measurements possible.

One suggestion for the origin of the α-poor stars is that these stars may have been accreted since the formation of the rest of the stellar halo. Smecker-Hane & Wyse (1992) and Gilmore & Wyse (1998) have suggested that dwarf galaxies or protogalactic fragments may have chemical enrichment histories with lower α-element enhancements. While it is not possible to determine absolutely the origin of individual field stars, the abundances of stars within potential future accretion targets (e.g., Milky Way satellite dwarf spheroidal [dSph] galaxies) should follow patterns similar to what Smecker-Hane & Wyse or Gilmore & Wyse suggest. The recent abundance analysis of Shetrone, Côté, & Sargent (2001) of stars within three nearby dSph galaxies allows such comparisons to be made in one potential source of accreted stars.

This paper will be organized as follows: In § 2 of this paper, we will calculate kinematic parameters for the F00 stars and select a sample for further study. The data will then be used to demonstrate that there exist correlations between abundance ratios and kinematics and that there are correlations between the element enhancements of certain light elements (§ 3). Finally, in § 4 we will show that true

analogues to the α-poor halo stars do not exist in the Milky Way satellite dSph galaxies studied to date.

2. DATA USED IN THE ANALYSIS

2.1. *Abundance Data*

The abundance ratios from F00 are presented in Figures 1–3. Also plotted are stars from several recent abundance surveys. As can be seen, there is significant overlap for metal-rich stars between the F00 data and the data of Edvardsson et al. (1993) and Clementini et al. (1999). In the extremely metal-poor regime ([Fe/H] $\lesssim -2$), the Ryan, Norris, & Bessell (1991) and the McWilliam et al. (1995) data provide more stars than F00, but the intermediate-metallicity range ($-2 <$ [Fe/H] < -1) is nearly exclusively covered by the F00 data.

Figure 4 presents comparisons of a few of the abundance ratios measured by both F00 and the other surveys. There is an overall good agreement between the F00 results and previous surveys, except for an $\sim$0.1 dex offset in [Si/Fe]. The origin of this offset is unclear—the atomic data used for Si by the different surveys all agree well, and the sensitivity of [Si/Fe] to systematic errors in the stellar parameters (see Table 8 of F00) is smaller than the values measured for other [X/Fe] ratios that do not show a similar offset.

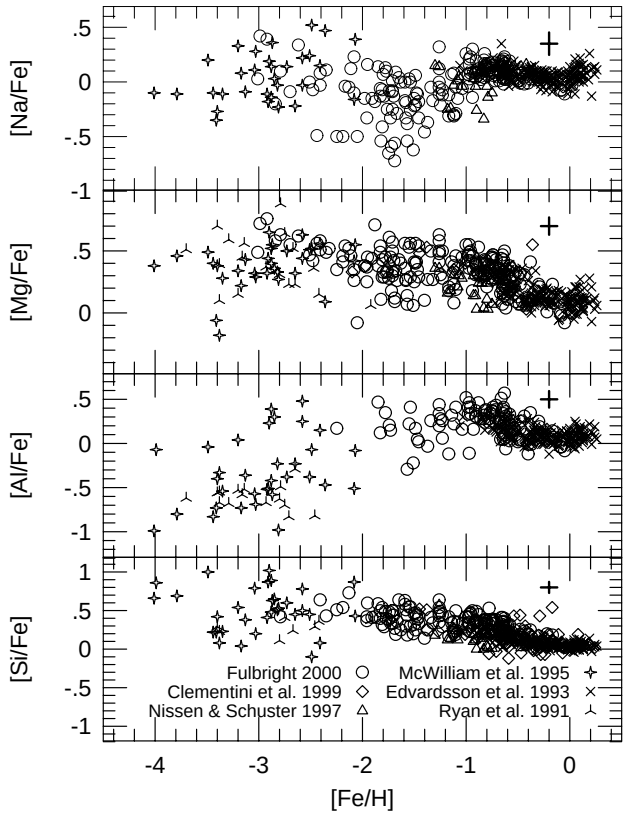

FIG. 1.—Distribution of [X/Fe] vs. [Fe/H] for Na, Mg, Al, and Si for the F00 and other recent abundance surveys. The estimated measurement errors for the F00 data are shown in the top right. The F00 star with low [X/Fe] at [Fe/H] = −2.05 for several panels in Figs. 1–3 is the star BD +80°245 (=HIP 40068), first studied by Carney et al. (1997).

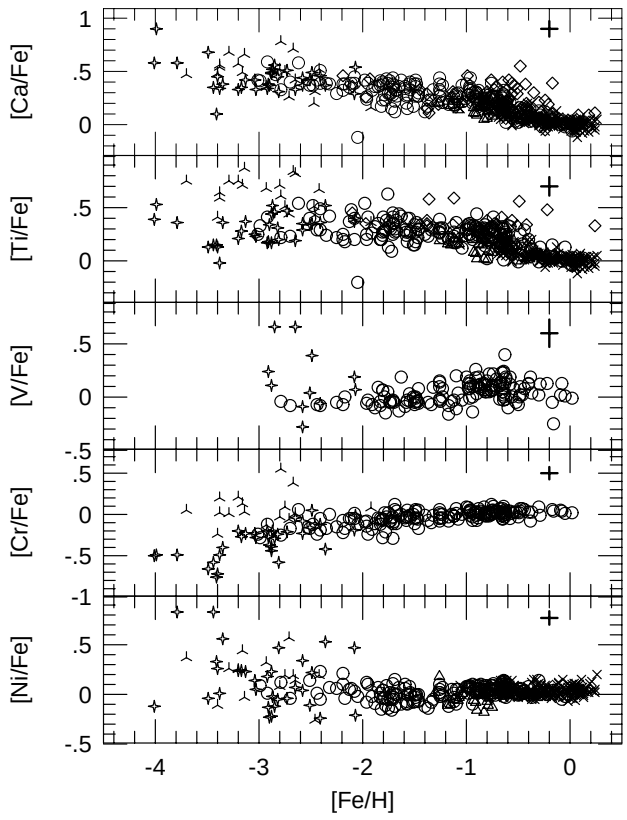

FIG. 2.—Same as Fig. 1, but for Ca, Ti, V, Cr, and Ni

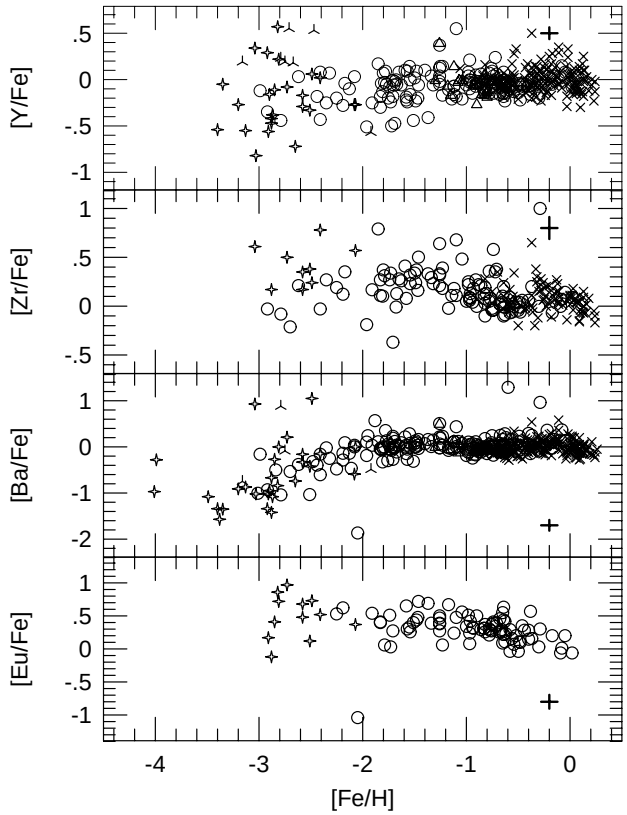

FIG. 3.—Same as Fig. 1, but for Y, Zr, Ba, and Eu. As mentioned in F00, the [Eu/Fe] measurement for BD +80°245 is an upper limit.

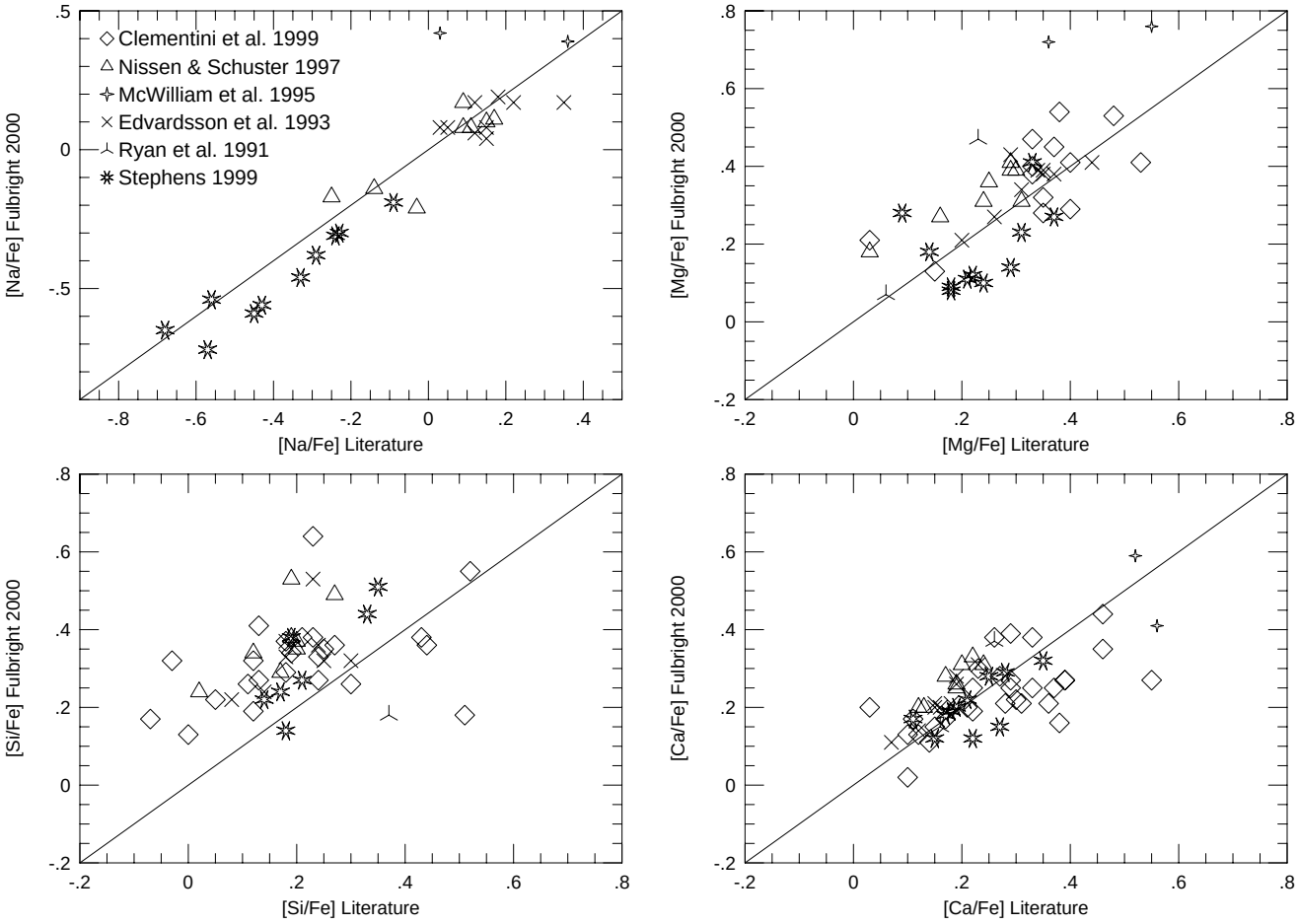

FIG. 4.—Comparison of the measured abundance ratios for stars in common between F00 and the other abundance surveys included in Figs. 1–3. As discussed in the text, the [Si/Fe] ratio shows a ~0.1 dex offset between the F00 and other surveys.

2.2. *Kinematic Data*

As stated in F00, one of the selection criteria for this survey is inclusion in the *Hipparcos* catalog (ESA 1997). All the proper motions and positions used in this survey come from the catalog. With the exception of several giants whose *Hipparcos* parallaxes are uncertain, all the adopted distances are derived from *Hipparcos* parallaxes. We adopt the H98 or Anthony-Twarog & Twarog (1994) distances (giving preference to H98) for those giants with *Hipparcos* $\delta(\pi)/\pi > 0.2$.

The adopted radial velocities (see Table 1) come from several sources, most often the Carney et al. (1994, hereafter CLLA) survey and the *Hipparcos* Input Catalog (HIC; ESA 1992). Other radial velocities were adopted from the literature. For the remaining stars, we measured radial velocities from the spectra themselves. No calibrations to radial velocity standards were made, but for the 73 stars in common with CLLA, the mean difference in the observed heliocentric radial velocity (F00 minus CLLA) is 0.3 ± 3.9 km s^{-1} (sdom), and for the 38 stars with radial velocities adopted from the HIC, the mean difference (F00 minus HIC) is 1.9 ± 4.4 km s^{-1}.

Given the above input parameters, the *UVW* velocities for the stars were calculated using a set of programs kindly provided by R. Hanson (1998, private communication). The *UVW* velocities are defined such that positive U values denote motion away from the Galactic center, positive V values are in the direction of the solar motion, and positive W values are parallel to the direction of the north Galactic pole. The *UVW* components were transformed to the local standard of rest (LSR) using the solar motion $(U_\odot, V_\odot, W_\odot)_{\rm LSR} = (-9, 12, 7$ km s$^{-1})$ (Mihalas & Binney 1981, p. 400). For purposes of this paper, the rotational velocity of the LSR with respect to the Galaxy was set to 220 km s^{-1}, and the galactocentric distance was set to 8.5 kpc. Also given in Table 1 are the galactic rest-frame velocities, $v_{\rm RF}$ $(= [U_{\rm LSR}^2 + (V_{\rm LSR} + 220)^2 + W_{\rm LSR}^2]^{1/2})$, orbital velocities in the direction of the Sun's orbit, $v_{\rm ROT}$ $(= V_{\rm LSR} + 220$ km s$^{-1})$, and specific angular momentum values, h $[= (v_{\rm ROT}^2 + W_{\rm LSR}^2)^{1/2}]$.

Orbital parameters for each star (maximum and minimum galactocentric radii, $R_{\rm max}$ and $R_{\rm min}$, maximum absolute distance from the galactic plane, $|Z_{\rm max}|$, and orbital eccentricity, e) were calculated using an integrator kindly provided by D. Lin (1999, private communication). The integrator uses a three-component potential describing the halo, disk, and bulge and is described in more detail by Johnston (1998). Each star was followed for 5 Gyr, or at least eight orbits. Table 1 lists the resulting kinematic and orbital parameter values. For completeness, the stars from S99 are listed with kinematic parameters from the CLLA

TABLE 1
KINEMATIC AND ORBITAL DATA

HIP[a]	RV (km s^{-1})	Ref.	U_{LSR} (km s^{-1})	V_{LSR} (km s^{-1})	W_{LSR} (km s^{-1})	v_{RF} (km s^{-1})	v_{ROT} (km s^{-1})	h (km s^{-1})	R_{min} (kpc)	R_{max} (kpc)	e	$\lvert Z_{max}\rvert$ (kpc)
Sun	...	...	−9	12	7	232	232	232	8.4	8.9	0.03	0.1
171	−36	1	−1	−59	−23	163	161	163	4.7	8.5	0.29	0.2
2413 ...	−378	4	−161	−345	−46	209	−125	−133	2.7	12.0	0.64	0.5
3026 ...	−49	2	−144	−223	−34	148	−3	34	0.0	10.4	0.99	0.4
3086 ...	−28	2	156	−42	55	243	178	186	4.3	12.8	0.49	0.7

NOTES.—Table 1 is available in its entirety in the electronic edition of the Astronomical Journal. A portion is shown here for guidance regarding its form and content.

[a] The first nine columns of data for the Stephens 1999 stars (those with Giclas numbers) are taken directly from the CLLA survey. The orbital parameters (R_{min}, R_{max}, e, and $\lvert Z_{max}\rvert$) were recalculated using the same galactic potential as the F00 stars.

REFERENCES.—(1) HIC; (2) Bond 1980; (3) CLLA; (4) Sandage & Fouts 1987; (5) F00 spectra; (6) Beers et al. 2000; (7) Norris 1986; (8) Chiba & Yoshii 1998; (9) Beers & Sommer-Larson 1995; (10) Bartkevicius et al. 1992; (11) Stetson 1983.

survey, but the orbital parameters were recalculated using the same galactic potential model as the F00 stars.

2.3. *Selection of Stars for Further Study*

An important kinematic parameter is the rest-frame velocity of the star with respect to the center of mass of the Galaxy (v_{RF}). Carney (1999) notes that the known α-poor stars show high galactic rest-frame velocities. If we wish to test whether this is true, we need to ensure that our sample does not exclude these important stars. In Figure 5, we plot [Fe/H] against v_{RF} and find that the F00 data set does not include a large number of very metal-poor ([Fe/H] < -2), high-velocity stars. This is most likely a selection effect, since the high-velocity star study of Carney, Latham, & Laird (1988) found that out of a sample of 24 stars with $v_{RF} > 375$ km s^{-1}, 13 have $-1 >$ [Fe/H] ≥ -2 and 10 showed [Fe/H] < -2. Most of the very metal-poor, high-velocity stars included in Carney et al. (1988) were too faint to be included in the F00 survey, and only the availability of the S99 data made it possible to include a reasonable number of high-velocity stars.

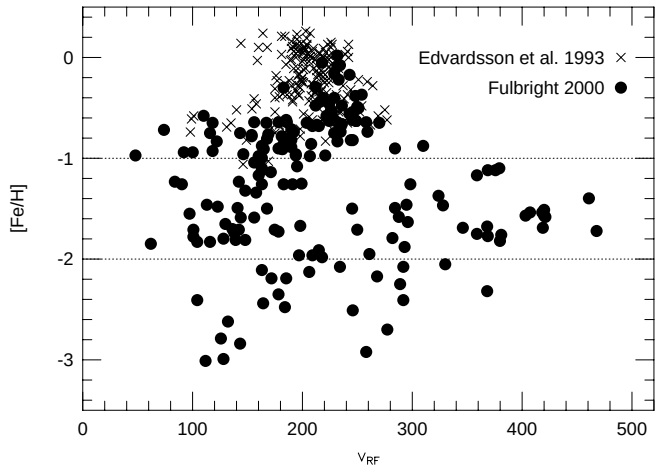

FIG. 5.—Distribution of [Fe/H] vs. v_{RF} for the F00 data. There is a lack of very metal-poor ([Fe/H] < -2), very high velocity stars, although such stars are known to exist. For the metal-rich ([Fe/H] > -1) stars, the F00 and Edvardsson et al. (1993) disk stars cover the same region, suggesting that the more metal-rich F00 stars are members of the disk population. The dotted lines denote the intermediate-metallicity selected sample.

Also included in Figure 5 are stars from the Edvardsson et al. (1993) sample of disk stars. As can be seen for the metal-rich stars ([Fe/H] > -1), the F00 and Edvardsson et al. (1993) samples share the same regions. Similar comparisons of the other kinematic and orbital parameters between the two samples in this metallicity range lead us to believe that the stars with [Fe/H] > -1 in the F00 sample are almost all members of the disk population.

Therefore, to ensure a less biased comparison of stars, we will generally confine our discussion of the relationship between kinematics and abundances to the 73 stars with $-1 <$ [Fe/H] < -2, as demarked by the dotted lines in Figure 5. For simplicity, we will refer to this set of stars as the "selected sample" for the remainder of the paper. Note that the selected sample does not include the well-known α-poor star BD +80°245.

3. ABUNDANCES AS A FUNCTION OF KINEMATIC PROPERTIES

3.1. [X/Fe] *versus* v_{RF}

In this section, we will test whether stars showing extreme orbital parameters show different abundance parameters than stars on more normal orbits. A useful kinematic parameter for these comparisons is v_{RF}, as defined above. This parameter is directly related to the star's kinetic energy with respect to the Galaxy. The value of v_{RF} is determined solely from observational data and, unlike R_{max}, is independent of the model used to describe the galactic gravitational potential.

As a quantitative way to describe any trends with v_{RF}, we fit least-squares lines to the distributions of [X/Fe] versus v_{RF} for the selected sample. In Figures 6 and 7, we plot the fits to the eight element ratios that are somewhat significant. For the fits involving Na, Mg, Al, Si, Ca, and Ni, the value of the correlation coefficients are such that there is a less than 0.05% chance that the correlations are random. For the fits involving Ti and Y, the probability is a few percent. These significance levels were confirmed by a nonparametric Spearman rank-order analysis, which compares only the rank order of the two variables and is independent of the form of the correlation. Fits to the other element ratios (including [Fe/H]) did not show any significant correlations. For simplicity, we will refer to the [X/Fe] ratios for Na, Mg, Al, Si, Ca, and Ni as the "varying" ratios.

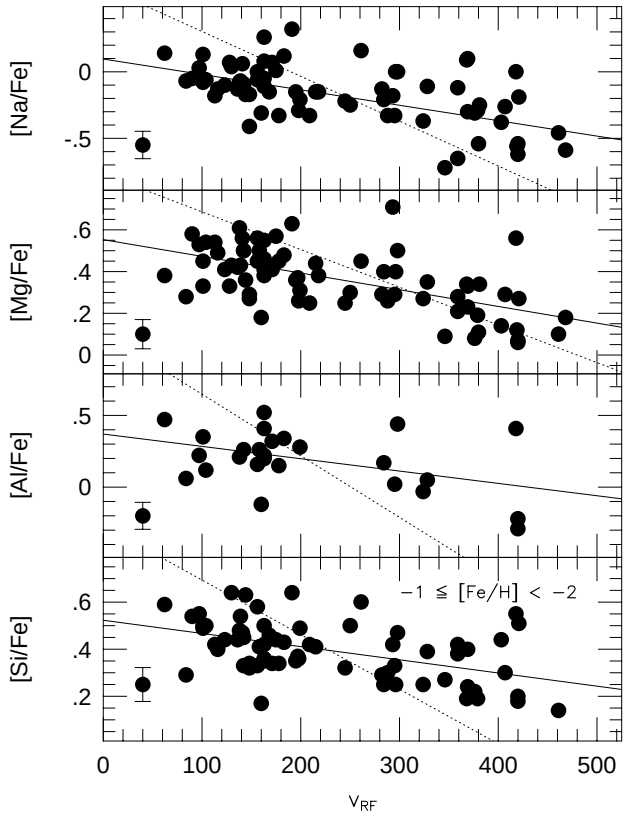

FIG. 6.—Plots of the distribution of [X/Fe] vs. v_{RF} for Na, Mg, Al, and Si for the selected sample. All four of these distributions show statistically significant correlations with respect to v_{RF}. The solid line is the least-squares fit to the data, while the dotted line is the reverse least-squares fit. The estimated measurement uncertainty for the abundance ratios is shown in the bottom left.

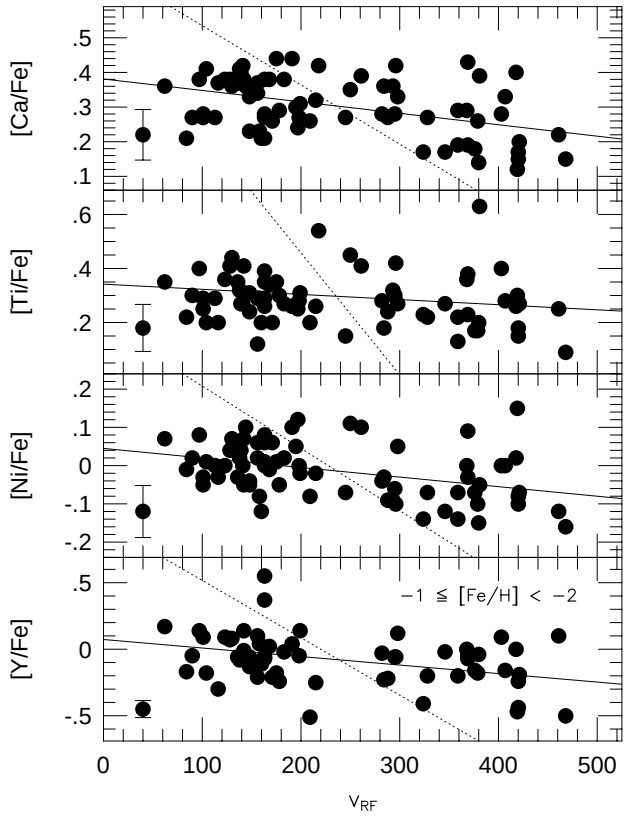

FIG. 7.—Same as Fig. 6, but for Ca, Ti, Ni, and Y. The correlations for Ti and Y are not as significant as the other six elements. The other elements studied in F00 (V, Cr, Zr, Ba, and Eu) do not show any statistically significant correlations with v_{RF}.

To further explore the potential relationship between [X/Fe] and v_{RF}, we divide the selected sample into three v_{RF} groups. The properties of these three groups are given in Table 2, and the mean values of [X/Fe] are plotted in Figure 8. The three groups have similar mean T_{eff} and [Fe/H] values, but the highest velocity group has a higher mean value of log g. This is due to the inclusion of the S99 stars to help fill out the highest velocity group. Even among metal-poor stars, high-velocity stars are rare. The S99 stars were specifically selected for their kinematics from the CLLA survey, which primarily included dwarf stars. The F00 survey selection was mainly based on metallicity, which allowed more evolved stars into the survey.

Figure 8 demonstrates that the highest velocity stars have a different distribution of light elements. The mean values of both [Na/Fe] and [Mg/Fe] are ~0.2 dex lower for the high-velocity group, while the mean values of [Al/Fe], [Si/Fe], [Ca/Fe], [Y/Fe], and [Ba/Fe] are slightly lower as well. The error bars in Figure 8 represent the standard deviation of the mean within each bin for that element ratio. They do not include the estimated random errors in the observations of the ratios (~0.1 dex, as discussed in F00).

Besides the relatively low light element abundance ratios, it is possible that the highest velocity stars also show slightly lower ratios of the *s*-process elements Y, Zr, and Ba. The mean [Ba/Eu] ratio does show a change between the velocity groups, but this measurement is limited by the number of Eu measurements. A lower *s*-process fraction in these stars would suggests that chemical evolution history of these stars contains less recycling of the ejecta from asymptotic giant branch stars, the suspected site of the main *s*-process. The size of the *s*-process deficiency is small and may not be significant, so an enlarged sample of high-quality, *s*-process element ratios should help clarify this picture.

3.2. *Element-Element Correlations*

The trends in Figures 6–8 suggest that the light element ratios may be correlated with each other. If this is the case, then [Na/Fe], which shows the largest range star-to-star variations in [X/Fe], could be used as a surrogate for describing the overall enhancements of these element ratios. Indeed, H98 and Sneden (1998) present evidence that there is a correlation between [Na/Fe] and [Mg/Fe] in halo giant stars. Here we attempt to expand this to other element ratios.

For the selected sample, we made linear least-squares fits to the [X/Fe] versus [Na/Fe] distributions. As a comparison, fits were also made to the [X/Fe] versus [Fe/H] distributions as well. We find strongly significant relationships between [Na/Fe] and the other varying ratios. Correlations significant to the few percent level were found for the fits with [Ti/Fe] and [Y/Fe]. For the fits using [Fe/H] as the independent variable, only [Cr/Fe] shows a strongly significant correlation. The above significance levels were confirmed through the use of Spearman rank-order tests.

TABLE 2
ABUNDANCE RATIOS AS A FUNCTION OF REST-FRAME VELOCITY FOR $-1 > [Fe/H] > -2$

	$v_{RF} < 150$			$150 < v_{RF} < 300$			$v_{RF} > 300$		
QUANTITY	Mean	sdom	n	Mean	sdom	n	Mean	sdom	n
T_{eff} (K)	5354	138	21	5218	85	31	5300	98	21
log g	3.1	0.3	21	3.2	0.2	31	4.0	0.2	21
[Fe/H]	−1.61	0.05	21	−1.49	0.06	31	−1.52	0.05	21
log n(Li)	+2.07	0.13	12	+1.55	0.16	17	+1.48	0.28	17
[Na/Fe]	−0.07	0.03	21	−0.10	0.03	30	−0.34	0.05	21
[Mg/Fe]	+0.44	0.02	21	+0.41	0.02	31	+0.22	0.03	21
[Al/Fe]	+0.24	0.05	7	+0.24	0.04	14	−0.02	0.13	5
[Si/Fe]	+0.47	0.02	20	+0.40	0.02	30	+0.31	0.03	17
[Ca/Fe]	+0.34	0.02	21	+0.32	0.01	31	+0.24	0.02	21
[Ti/Fe]	+0.31	0.02	20	+0.29	0.02	31	+0.26	0.03	21
[V/Fe]	−0.01	0.05	7	+0.00	0.02	27	−0.02	0.10	8
[Cr/Fe]	−0.08	0.02	20	−0.04	0.01	30	−0.02	0.01	21
[Ni/Fe]	+0.01	0.01	21	+0.00	0.01	30	−0.06	0.02	21
[Y/Fe]	−0.02	0.04	16	−0.05	0.04	24	−0.17	0.04	19
[Zr/Fe]	+0.25	0.08	13	+0.26	0.05	21	+0.19	0.05	6
[Ba/Fe]	+0.08	0.04	21	+0.07	0.03	30	−0.02	0.03	21
[Eu/Fe]	+0.36	0.05	7	+0.41	0.05	15	+0.44	0.06	6
[Y/Zr]	−0.29	0.06	13	−0.32	0.03	21	−0.35	0.10	6
[Ba/Eu]	−0.21	0.11	7	−0.40	0.06	15	−0.49	0.07	6
v_{RF} (km s^{-1})	120	5	21	212	9	31	389	8	21
v_{ROT} (km s^{-1})	47	18	21	39	20	31	−108	43	21
h (km s^{-1})	43	20	21	42	24	31	−88	57	21
R_{max} (kpc)	9.1	0.1	21	14.3	2.4	31	37.4	3.1	21
$\|Z_{max}\|$ (kpc)	0.6	0.1	21	3.1	2.2	31	6.2	1.9	21
e	0.72	0.04	21	0.66	0.05	31	0.76	0.05	21

Another confirmation comes from the relative size of the standard deviations of the [X/Fe] values around the least-squares fits ($\sigma_{[X/Fe]}$). For the five ratios that strongly correlate with [Na/Fe], the values of $\sigma_{[X/Fe]}$ found for the fit to [Na/Fe] are ~30% smaller than those found for the fit to [Fe/H]. For the remaining ratios, the $\sigma_{[X/Fe]}$ values were comparable between the fits and the different independent variables.

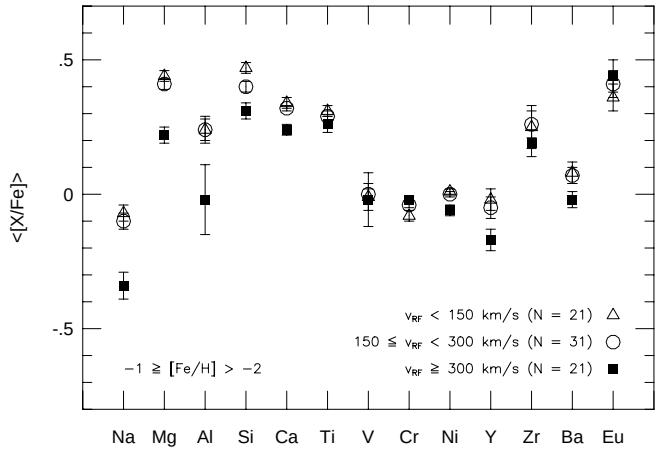

FIG. 8.—Plots of the mean value of [X/Fe] for the selected sample broken into three v_{RF} groups. The highest velocity group has significantly lower mean values for several elements. Note that the number of measurements for any given ratio may be smaller than the number of stars in that group. This is especially a problem for Al, which helps explain the large sdom error bars for that ratio.

In Figure 9, we plot the [X/Fe] versus [Na/Fe] distributions for the four α-elements studied in F00. All four ratios show trends with [Na/Fe], but as a further test, we calculated the value of [α/Fe] (the mean of the [X/Fe] ratios for Mg, Si, Ca, and Ti) for the 65 stars in the selected sample having abundance measurements for all four elements. The plot of [α/Fe] versus [Na/Fe] is presented in the top panel of Figure 10. The quality of the fit and the statistical significance is better than the fits to the individual ratios themselves. Also plotted in Figure 10 are the [X/Fe] versus [Na/Fe] distributions and fits for Al, Ni, and Y.

Random and systematic errors in the stellar parameters (T_{eff}, log g, etc.) could possibly lead to the correlations seen here. Table 8 of F00 gives the effects of specific changes in the stellar parameters on the final abundance ratios. For most of the varying elements, the sign of the changes all match, meaning that the errors are correlated. However, the magnitude of the changes are too small with respect to the variations seen in the elements. For example, a change of 150 K in T_{eff}, a 0.2 dex change in log g, or a 0.3 km s^{-1} change in the microturbulent velocity results in a change of ~0.05 dex or less in the resulting abundances. The change in parameter values needed to explain the range of [X/Fe] values seen in unreasonable. In addition, the lines used in F00 were specifically chosen to ensure that the individual lines of a given element have consistent results as compared with the other lines of that element over a wide range of stellar parameters. Because of the care taken to form the line list, it is unlikely, short of problems with the basic assumptions of the LTE plane-parallel analysis, that the results seen here are artifacts of line selection or the abundance analysis.

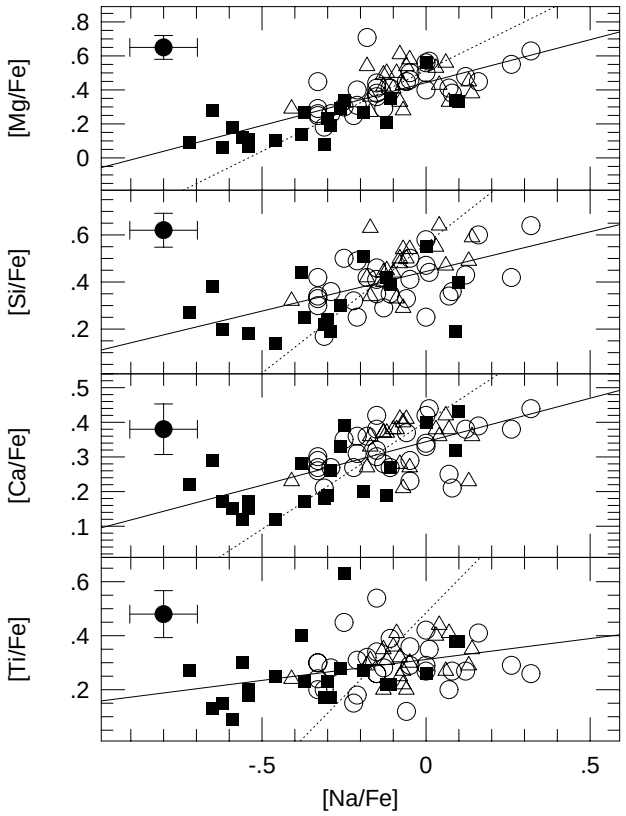

FIG. 9.—Plots of the correlation between the [X/Fe] ratios for the four α-elements measured in F00 and [Na/Fe]. The symbols are the same as in Fig. 8, and the error bars denote the estimated measurement uncertainty for the ratios. As in Figs. 6 and 7, the solid line marks the least-squares fit to the data, while the dotted line is the reverse fit. The displacement of the high-velocity stars to lower [X/Fe] values is clear in these plots.

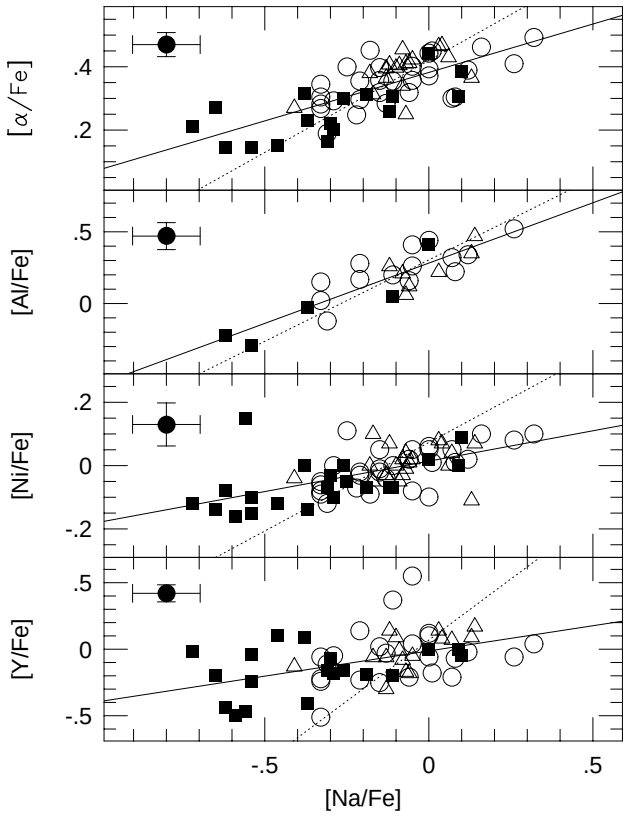

FIG. 10.—Same as Fig. 9, but for the mean α-element abundance (for only the 65 stars with measurements of all four elements), Al, Ni, and Y. The statistical significance of the [α/Fe] vs. [Na/Fe] correlation is greater than any of the four individual α-elements with [Na/Fe].

3.3. *Abundances and Orbital Parameters*

Instead of using v_{RF} as the kinematic parameter, Carney et al. (1997) and Carney (1999) noted potential trends between R_{max} or h and abundances. Using [Na/Fe] as a surrogate for the other varying element ratios, we can test these trends with the F00 data set. Plots of [Na/Fe] against orbital parameters are shown in Figures 10*a*–10*c*. The fraction of "Na-poor" stars (those with [Na/Fe] < -0.36) increases for $R_{max} > 20$ kpc (9 of 22 stars) and $|Z_{max}| > 5$ kpc (5 of 10 stars; see Fig. 11). From these counts, about a half of extreme halo stars should show lower element ratios. Conversely, 55% (6 of 11) of stars with [Na/Fe] < -0.36 have $R_{max} > 40$ kpc, while only 6% of the remaining sample has values of R_{max} this high. Ten of the 11 Na-poor stars have $v_{RF} > 300$ km s^{-1}, while only 11 of the 113 other stars have this high a value of v_{RF}.

Carney (1999) suggested that the previously observed α-poor stars also had high "specific angular momentum" (h) values. For any star, the maximum value of $|h|$ is v_{RF}. For the 11 stars with [Na/Fe] < -0.36, the mean value of $|h|/v_{RF}$ is 0.78 ± 0.07 (sdom). If the one star (G197-30) with an $|h|/v_{RF}$ value of 0.17 is eliminated, the mean value increases to 0.84 ± 0.04. This compares with a mean value of 0.66 ± 0.04 for the other 61 stars in the selected sample with [Na/Fe] abundances.

4. ACCRETION ORIGIN OF THE α-POOR STARS?

So far, we have shown that the highest velocity stars in the solar neighborhood show a different pattern of abundance ratios than the lower velocity stars. This suggests that these stars did not form in the same manner as the rest of the halo. One theory for the origin of the low-α halo stars is that they were accreted from the cannibalization of other stellar systems. If the stellar halo of the Milky Way was made up of disrupted and accreted protogalactic fragments, as suggested by Côté et al. (2000), then studies of stars within present-day dwarf galaxies (assuming they are products of similar fragments) may help explain the abundance patterns seen in the halo. Shetrone et al. (2001) analyzed high-resolution spectra of 17 giants stars in the Draco, Ursa Minor, and Sextans dSph galaxies. Their methodology is similar to the LTE analysis technique employed by F00, although the spectra were of lower S/N ($\sim$15–35) than F00.

In Figure 12, we plot the mean [X/Fe] values for the 10 Shetrone et al. (2001) dSph stars with $-1 >$ [Fe/H] ≥ -2, along with the three kinematic groups of the selected-sample stars. For several elements, the mean values of the [X/Fe] ratios differ between the dSph stars and the halo stars. It is also clear that the dSph abundance pattern does not match what is seen in α-poor stars. For example, the most extreme α-poor star known, BD $+80°245$ (=HIP 40068) shows [Ba/Fe] and [Eu/Fe] ratios $\sim$1.5 dex below halo stars of similar metallicity (see Fig. 3). This would place it off the bottom of Figure 12, while the mean dSph values for these two ratios is higher than the mean halo value.

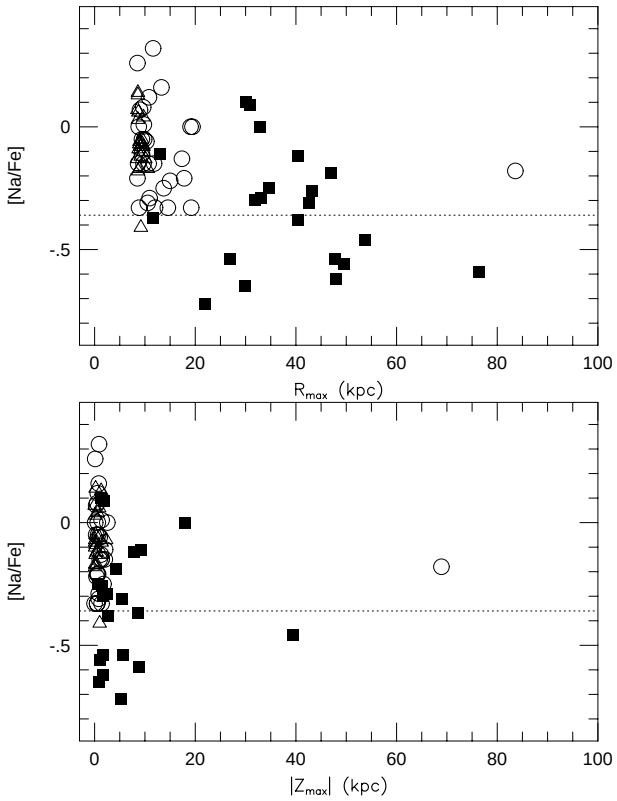

FIG. 11.—Value of [Na/Fe] as a function of R_{max} and $|Z_{max}|$ for the selected sample. The symbols are the same as in Fig. 8, and the dotted line denotes the mean [Na/Fe] ratio of the highest v_{RF} group ([Na/Fe] = −0.36). Approximately half of the stars with $R_{max} > 20$ kpc or $|Z_{max}| > 5$ kpc show [Na/Fe] ratios lower than nearly all the lower v_{RF} halo stars.

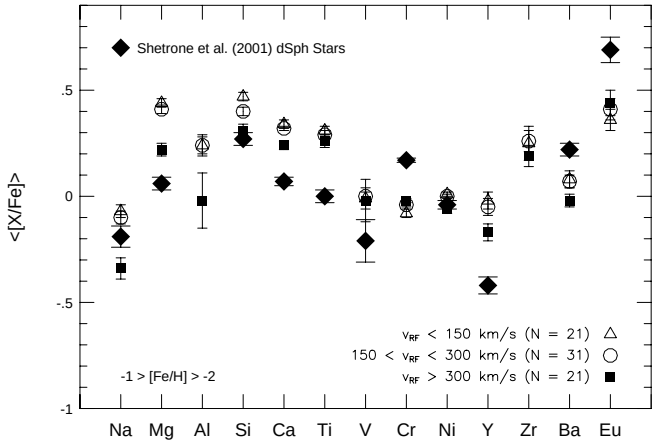

FIG. 12.—Same as Fig. 8, but with the mean [X/Fe] ratios for the intermediate-metallicity dSph stars from Shetrone et al. (2001) plotted as well. While the dSph stars show similar mean values to the high-velocity stars for some elements, the large differences seen in the mean ratios for Ca, Ti, Cr, Y, Ba, and Eu strongly suggest that the high-velocity stars were not accreted from disrupted dSph galaxies like the ones observed by Shetrone et al. (2001).

Since the F00 survey did not find any stars with abundance patterns similar to the dSph stars, it is unlikely that a large fraction of the field halo stars in the solar neighborhood, including the α-poor stars, are former members of dSph galaxies of the kind studied by Shetrone et al. (2001).

Despite this, continued high-resolution work on individual stars in other galaxies may find an extragalactic origin for the α-poor stars. For example, Hill et al. (2000) present O and Al abundances derived from high-quality, high-resolution spectra of 10 giants in globular clusters associated with the LMC. For the stars that do not show signs of deep mixing (enhanced [Al/Fe] and depressed [O/Fe]), the general trend of the metal-poor stars is to have low values of [O/Fe] and [Al/Fe] compared with unmixed Galactic globular cluster giants. The analysis of a full range of elements in the stars is necessary before further comparisons can be made. However, one exciting prospect is that the LMC cluster system shows a range of ages (see Elson & Fall 1988 and Geisler et al. 1997), so it may be possible to explore the effects of time of formation on abundance ratios.

5. DISCUSSION AND FUTURE WORK

In this paper, we have presented observational evidence that shows that the [X/Fe] ratios for certain elements decline in concert for higher values of v_{RF}. Here we discuss some possible scenarios that may produce the pattern of elements found in the high-velocity stars.

The production of Na and Mg by Type II supernova is dominated by massive progenitor stars with $M > 30\ M_{\odot}$ (see Fig. 6 of McWilliam 1997 and Woosley & Weaver 1995), while the lower mass progenitors create relatively more of the heavier α- and Fe-group elements. A possible explanation for the decline of the light elements without a similar decline in the heavier elements is to decrease the relative fraction of very massive stars in the chemical enrichment history of the α-poor stars. The connection of initial mass function (IMF) slope to location in the Galactic potential (assuming that the stars with higher v_{RF} formed at greater distances from the Galactic center) is unclear.

Another possibility is incomplete mixing. Using a single Salpeter IMF, Argast et al. (2000) ran simulations of the chemical enrichment history of the early Galaxy and included provisions for incomplete mixing. They found that incomplete mixing can explain the presence of star-to-star variations for the light element ratios for the moderately metal-poor stars, but if the mixing in the halo was less complete at high v_{RF}, one would expect to see high-velocity stars with relatively high values of [Na/Fe], [Mg/Fe], etc., as well.

Alternatively, the lower [X/Fe] ratios for some elements may be due to extra Fe-rich material being added to the gas that formed the stars that are now at high v_{RF}. Type Ia supernovae could be the source of the Fe-group enrichment. There are, however, a few observational details that do not agree with this theory:

First, other element ratios like [Ca/Fe] and [Ti/Fe] do not show the same level of decrease with v_{RF}. Nucleosynthesis models of Type Ia supernovae do suggest these events create a reasonable amount of Ca and Ti (Nomoto et al. 1997), but it is unclear whether or not these kind of events can keep the mean [Ti/Fe] value approximately constant. Second, these same models predict an overproduction of Ni with respect to Fe by Type Ia supernovae. If anything, the mean [Ni/Fe] ratio in the high-velocity stars is lower than for the rest of the halo (see Fig. 8).

Some of these issues could possibly be resolved by careful analysis of additional elements. Oxygen, for example, should be formed mainly by the very massive Type II supernovae. That means the [O/Fe] ratio should track [Na/Fe] and [Mg/Fe]. By a similar argument, [S/Fe] should follow [Si/Fe]. There may also be clues in the other Fe-group and heavier elements on the relative contributions of Type Ia and II supernovae. We are in the process of analyzing many of these elements in the F00 spectra.

Another natural next step is to observe more high-velocity stars, such as those listed in Carney et al. (1988) or elsewhere in the literature. The 11 star survey of S99 found seven Na-poor stars using kinematic selection criteria. These stars are rare and therefore faint and require time on 8 to 10 m class telescopes to build up a sizable sample. However, it is also important to continue observing lower velocity stars in order to search for Na-poor stars in their midst. It is paramount to resolve the potential non-LTE effects in the abundance analysis through either consistent sample selection or, preferably, accurate stellar atmosphere modeling. Finally, it cannot be stressed enough that any such new survey needs to follow some sort of self-consistent analysis procedure for all the stars, even if it is not the same one followed in F00. Any procedure should also include the analysis of a wide sample of stars for comparisons, as for this type of work, accurate relative abundances are more important than the absolute overall scaling.

6. SUMMARY OF RESULTS

From the analysis of the self-consistent abundance analysis of F00, combined with *Hipparcos*-based kinematics, we have found the following:

1. The general trends of the element-to-iron ratios with respect to [Fe/H] are similar to those seen by previous studies.
2. For intermediate-metallicity ($-2 < [Fe/H] < -1$) stars from F00, the [X/Fe] ratios for Na, Mg, Al, Si, Ca, and Ni, as well as possibly Ti and Y, show a decrease in the value of [X/Fe] with increasing v_{RF}.
3. For the metal-poor stars the values of [X/Fe] for the above elements are correlated. The correlation between [α/Fe] and [Na/Fe] is show a higher significance than between any of the individual [X/Fe] ratios and [Na/Fe].
4. When compared with the field halo sample, the dSph giant sample of Shetrone et al. (2001) shows a different pattern of abundance ratios than the field halo sample, including the high v_{RF} stars. It is unlikely that the α-poor stars in the solar neighborhood originated the dSph galaxies similar to those studied by Shetrone et al. (2001).

The papers of this series make up the Ph.D. thesis of J. P. F. at the University of California, Santa Cruz. J. P. F. wishes to thank the members of his committee (R. Kraft, R. Peterson, M. Bolte, and P. Gahathakurta) for their efforts and advice. J. P. F. also wishes to thank B. Hanson for his assistance with the *Hipparcos* catalog and the codes for calculating *UVW* components for the sample stars, D. Lin for the codes used in calculating the orbits of the sample stars, and J. Johnson and V. Weafer for reviewing drafts of this paper. Special thanks should go to the anonymous referee for useful comments. This research was supported by NSF contract AST 96-18351 to R. P. Kraft and by the National Research Council of Canada.

REFERENCES

Anthony-Twarog, B. J., & Twarog, B. A. 1994, AJ, 107, 1577
Argast, D., Samland, M., Gerhard, O. E., & Thielemann, F.-K. 2000, A&A, 356, 873
Bartkevicius, A., Sperauskas, J., Rastorguev, A. S., & Tokovinin, A. A. 1992, Baltic Astron., 1, 47
Beers, T. C., Chiba, M., Yoshii, Y., Hanson, R. B., Fuchs, B., & Rossi, S. 2000, AJ, 119, 2866
Beers, T. C., & Sommer-Larsen, J. 1995, ApJS, 96, 175
Bond, H. E. 1980, ApJS, 44, 517
Brown, J. A., Wallerstein, G., & Zucker, D. 1997, AJ, 114, 180
Carney, B. W. 1999, in ASP Conf. Ser. 165, The Third Stromlo Symposium: The Galactic Halo, ed. B. K. Gibson, T. S. Axelrod, & M. E. Putman (San Francisco: ASP), 230
Carney, B. W., Latham, D. W., & Laird, J. B. 1988, AJ, 96, 560
Carney, B. W., Latham, D. W., Laird, J. B., & Aguilar, L. A. 1994, AJ, 107, 2240 (CLLA)
Carney, B. W., Wright, J. S., Sneden, C., Laird, J. B., Aguilar, L. A., & Latham, D. W. 1997, AJ, 114, 363
Chiba, M., & Yoshii, Y. 1998, AJ, 115, 168
Clementini, G., Gratton, R. G., Carretta, E., & Sneden, C. 1999, MNRAS, 302, 22
Côté, P., Marzke, R. O., West, M. J., & Minniti, D. 2000, ApJ, 533, 869
Edvardsson, B., Andersen, J., Gustafsson, B., Lambert, D. L., Nissen, P. E., & Tomkin, J. 1993, A&A, 275, 101
Elson, R. A. W., & Fall, S. M. 1988, AJ, 96, 1383
ESA. 1992, The Hipparcos Input Catalogue (ESA SP-1136) (Noordwijk: ESA)
———. 1997, The Hipparcos and Tycho Catalogues (ESA SP-1200) (Noordwijk: ESA)
Fulbright, J. P. 2000, AJ, 120, 1841 (F00)
Geisler, D., Bica, E., Dottori, H., Claria, J. J., Paitti, A. E., & Santos, J. F. C., Jr. 1997, AJ, 114, 1920
Gilmore, G., & Wyse, R. F. G. 1998, AJ, 116, 748
Hanson, R. B., Sneden, C., Kraft, R. P., & Fulbright, J. P. 1998, AJ, 116, 1286 (H98)
Hill, V., François, P., Spite, M., Primas, F., & Spite, F. 2000, A&A, 364, L19
Johnston, K. V. 1998, ApJ, 495, 297
King, J. R. 1997, AJ, 113, 2302
McWilliam, A. 1997, ARA&A, 35, 503
McWilliam, A., Preston, G. W., Sneden, C., & Searle, L. 1995, AJ, 109, 2757
Mihalas, D., & Binney, J. 1981, Galactic Astronomy: Structure and Kinematics (2d ed.; San Francisco: Freeman)
Nomoto, K., Iwamoto, K., Nakasato, N., Thielemann, F.-K., Brachwitz, F., Tsujimoto, T., Kubo, Y., & Kishimoto, N. 1997, Nucl. Phys. A, 621, 467
Norris, J. 1986, ApJS, 61, 667
Ryan, S. G., Norris, J. E., & Bessell, M. S. 1991, AJ, 102, 303
Sandage, A., & Fouts, G. 1987, AJ, 93, 74
Shetrone, M. D., Côté, P., & Sargent, W. L. W. 2001, ApJ, 548, 592
Smecker-Hane, T. A., & Wyse, R. F. G. 1992, AJ, 103, 1621
Sneden, C. 1998, in IAU Symp. 187, Cosmic Chemical Evolution, ed. J. W. Truran & K. Nomoto (Dordrecht: Kluwer), in press
Stephens, A. 1999, AJ, 117, 1771 (S99)
Stetson, P. B. 1983, AJ, 88, 1349
Tinsley, B. M. 1979, ApJ, 229, 1046
Woosley, S. E., & Weaver, T. A. 1995, ApJS, 101, 181